8

WAVE INDUCED BENDING MOMENTS ON LONG FLOATING BEAMS.

F.P. Lockett, A.M. Peatfield, M.J. West.

Sea Energy Associates-
Lanchester Polytechnic Wave Energy Research Group.
Priory Street, Coventry, England.

SYNOPSIS.

The paper describes how the Sea Energy Associates-Lanchester Polytechnic Wave energy research group have, over the last six years, used model tests to investigate wave induced bending moments in long floating beams. A development of a semi-empirical, quasi-static, mathematical model, using a simplified transfer function to define the interaction between wave and structure, is explained.

Comparisons of the quasi-static predictions and the maximum measured bending moments over a wide range of beam lengths, stiffnesses and section shapes show good agreement within the likely spread of sea state parameters.

Graphs are presented which enable predictions to be made of maximum bending moments in long, low freeboard, floating beams situated in a defined sea state.

INTRODUCTION.

A number of designs of wave energy extracting devices at present under investigation in the United Kingdom have, as their principal structural member, a long floating beam, or spine, upon which equipment for energy extraction is mounted. These spine based devices are designed to operate in a full range of orientations, from the 'terminator' position, where the spine lies nearly perpendicular to the principal wave direction, to the 'attenuator' position, with the spine parallel to the principal wave direction.

WAVE INDUCED BENDING MOMENTS ON LONG FLOATING BEAMS.

As the energy extraction efficiency of such devices depends partly upon the stability of the spine, relative to the wave movements, it is important that the spine be made as long as possible in the light of the wave induced bending moments and the strength of suitable construction materials. Currently proposed lengths are about 300 m.

Thus the Sea Energy Associates-Lanchester Polytechnic group at Coventry have, over the past six years, carried out an extensive series of model tests in natural environments, at scales ranging from 1/50th. to 1/10th., in order to establish a reliable method of predicting wave induced bending moments in long, low freeboard, floating beams.

A semi-empirical approach has been followed in which the measured bending moments from tests on beams of varying shapes, lengths and stiffnesses have been compared with those predicted from a simple quasi-static mathematical model which uses an empirical wave to spine loading transfer function derived from narrow wave tank force measurements carried out by Stephen Salter at the University of Edinburgh.

The quasi-static model considers the bending moments induced by a single idealised wave of known height, wave length and 'crest' length parallel to the longitudinal axis of the beam. The worst case bending moment is shown to be dependent on the 'crest' length to spine length ratio.

In a real sea condition although the wave height and period distribution can be reasonably well defined, the 'crest' length distribution is a function of the wave directionality and is not easily defined without extensive, and expensive, wave measurements. However, despite this difficulty, the comparison between the maximum measured bending moments and those calculated from the quasi-static analysis is good and the authors have confidence that, within the accuracy of the sea state definition, this method can be used to predict design loadings for full scale floating beams.

SCALE MODEL TESTS.

The model tests carried out by the SEA-Lanchester team were largely dictated by the requirements of the proposed full scale wave energy device and the wave climate available for testing. As no wide wave tank was available, it was decided to carry out tests in a local reservoir which had a naturally occurring wave climate of approximately 1/50th. scale of a line forward of centre on the expected North Atlantic scatter diagram. A more extensive series of tests were also carried out in Loch Ness, Scotland, which has about a 1/10th. scale wave climate.

WAVE INDUCED BENDING MOMENTS ON LONG FLOATING BEAMS.

As initially the work was concerned with the development of the Salter duck device, most of the tests were on a series of round section spines ranging in length from 500 m. to 240 m. at full scale. However in the last three years, work has moved on to the Clam wave energy device and tests have been carried out on spines with nearly rectangular sections and of lengths ranging from 650 m. to 270 m. at full scale.

The mooring arrangement has generally been by a 'V' yoke harness from the spine quarter points to an anchored leading buoy, which allows the spine to self-align to the principal wave direction at an angle controlled by the relative lengths of the 'V' yoke arms. Tests have been carried out with the spine at angles to the principal wave direction ranging from 90 degrees to 0 degrees, the in line position. It has been established that the peak mooring forces, particularly when compliant mooring rodes are used, have less than a 5% effect on the peak bending moments.

Most of the spines tested have had a small freeboard to draught ratio, about 1 : 7, but one series of tests has been carried out with an extended freeboard, rectangular spine giving a ratio of about 1 : 3.5.

Measurements of wave height, spine strain, spine movement and mooring forces have been recorded over thousands of 384 second test runs and values of mean, r.m.s. and peaks calculated. The complete results of the full range of tests have been, or are being, reported in the SEA-Lanchester wave energy research group reports to the Energy Technology Support Unit of the Department of Energy.

THE QUASI-STATIC MATHEMATICAL MODEL.

The rigorous theoretical solution of the wave induced forces on an immersed body is a difficult problem, particularly when considering extreme sea conditions.

Our approach has been to start with Salter's[1] two dimensional experimental estimates of wave forces, then to argue theoretical modifications to these forces due to body motion and deformation, and hence calculate the response of a long floating beam which moves and bends in vertical and horizontal directions under wave loads.

Salter's experiments measured, in a narrow wave channel, the sinusoidally varying vertical and horizontal forces experienced by a fixed immersed body of constant section in monochromatic progressive waves.

He suggested the simple formula:-

$$F \text{ / unit length} = \rho g C_f D \times 2a \qquad (1)$$

for the maximum wave force. Where ρ = water density, g = acceleration due to gravity, a = maximum wave amplitude.

Salter found that equation (1) applied for both vertical and horizontal forces with the appropriate force coefficients, C_f, and the relevant projected dimension, D, of the immersed body; in the horizontal plane for vertical forces and in the vertical plane for horizontal forces. Equation (1) refers to a body fixed in the water; body movement in the wave will clearly affect the force.

The assumption is made that if the floating body moves a distance d, from its still water equilibrium position in a wave of instantaneous amplitude e, then the force 'seen' by the body is $2(e-d)\ \rho g C_f D$. So for a body motion and/or deformation of amplitude y, in phase with a wave of amplitude a, the maximum predicted force is thus modified to:-

$$F \text{ / unit length} = \rho g C_f D(2a-2y)$$

which becomes:-

$$F \text{ / unit length} = \rho g C_f D(H-2y) \qquad (2)$$

Where H = 2a = peak to trough wave height.

Calculations show that, providing the cross sectional dimensions are small compared with the wave length, the body response motion is approximately in phase with the wave motion, ie. inertia effects are small.

So assuming that (2) applies to individual sections of spine along its length, the maximum spine movement, y(x), at distance x from its centre, measured from its still water equilibrium position, due to an incident wave $H\cos\left(\frac{2\pi x}{\lambda c} - \phi\right)$ (representing an asymmetric, monochromatic crossed sea of 'crest' length = distance between successive peaks, measured along the spine, = λ_c) is given by the beam equation:-

$$\frac{d^2}{dx^2}\left(EI\ \frac{d^2y}{dx^2}\right) = \rho g C_f D\ \left(H\cos\left(\frac{2\pi x}{\lambda_c} - \phi\right) - 2y\right) \qquad (3)$$

with boundary conditions to give zero bending moment and shear force at the spine ends.

Thus the boundary conditions dictate that the spine always moves to a position of static equilibrium in which the net wave force and moment of force on the spine are zero.

Thus for our estimation of spine bending loads we are supposing that the dynamic spine response is an oscillation with the wave, the

spine motion amplitude, y(x), being given by the 'static' equation (3). We call this analysis 'Quasi-Static'.

Solutions to equation (3), both for the symmetric (ϕ=0) and assymmetric cases, have been produced, initially by analogue but more recently by digital methods, for a range of EI values and 'crest' length to spine length ratios, λ_c/L.

Digital solutions have been used to evaluate the maximum predicted bending moment and shear force in the general, monochromatic, asymmetric wave loading conditions. The analysis shows that the largest bending moment occurs at the spine centre under symmetric loading with $\lambda_c = 0.9$ L. (The position of the peak is actually an insensitive function of EI.) For positions between the spine centre and ends, asymmetric loading always produces greater moments for a particular wave height and 'crest' length.

For ease of presentation and use for a wide range of beams the results have been parameterized by the spine constant $U = \rho g C_f D L^4/EI$, a given curve being applicable for an appropriate value of U.

Figure 1 is the universal curve for evaluating the maximum spine centre bending moment parameter, $B.M./(\rho g C_f D H L^2/16)$, from the stiffness parameter $EI/C_f D L^4$, for the 'crest' length to spine length ratio, $\lambda_c/L = 0.896$. Figure 2 shows curves, for a range of stiffnesses, of the bending moment parameter for all positions along the spine. Figure 3 shows curves, for a range of stiffnesses, of the spine centre bending moment parameter against values of λ_c/L.

EXPERIMENTAL RESULTS

Plots of the peak bending moments measured from the experimental tests at 1/50th. and 1/10th. scale against the significant wave height, H_s, showed an approximately linear increase with wave height up to a limiting condition. The peak bending moment levelled off and then reduced as the wave height increased further.

In order to evaluate predicted bending moments from the quasi-static analysis some assumptions had to be made concerning the characteristics of the wave causing the peak bending moment. As the wave climates of both 1/50th. and 1/10th. scale were locally generated wind seas, with some topographical restrictions at 1/10th. scale, the directional spread was not high. From photographic and television observations it was estimated that the 'crest' length to wave length ratio was rarely less than about 3 : 1 and thus it was assumed that generally the minimum 'crest' length to wave height ratio in a 384 second record was about 30 : 1. It was also assumed that one of the largest waves likely to occur, within the record period, would have a 'crest' length approximately 30 x wave height. Using the Longuet-Higgins distribution, the most likely maximum wave

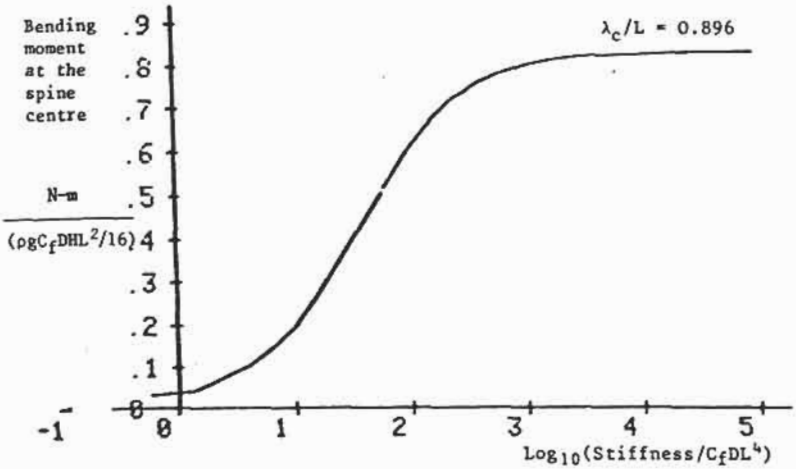

FIGURE 1 BENDING MOMENT-STIFFNESS UNIVERSAL CURVE

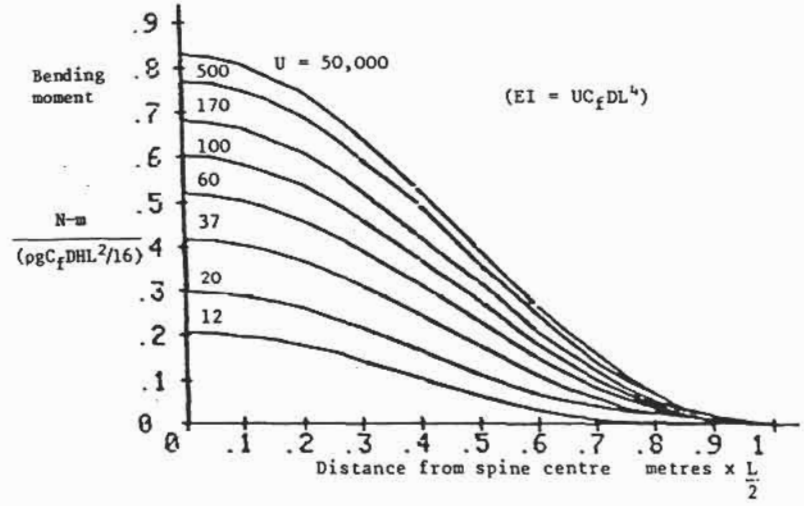

FIGURE 2 BENDING MOMENT ALONG THE SPINE FOR A RANGE OF STIFFNESSES

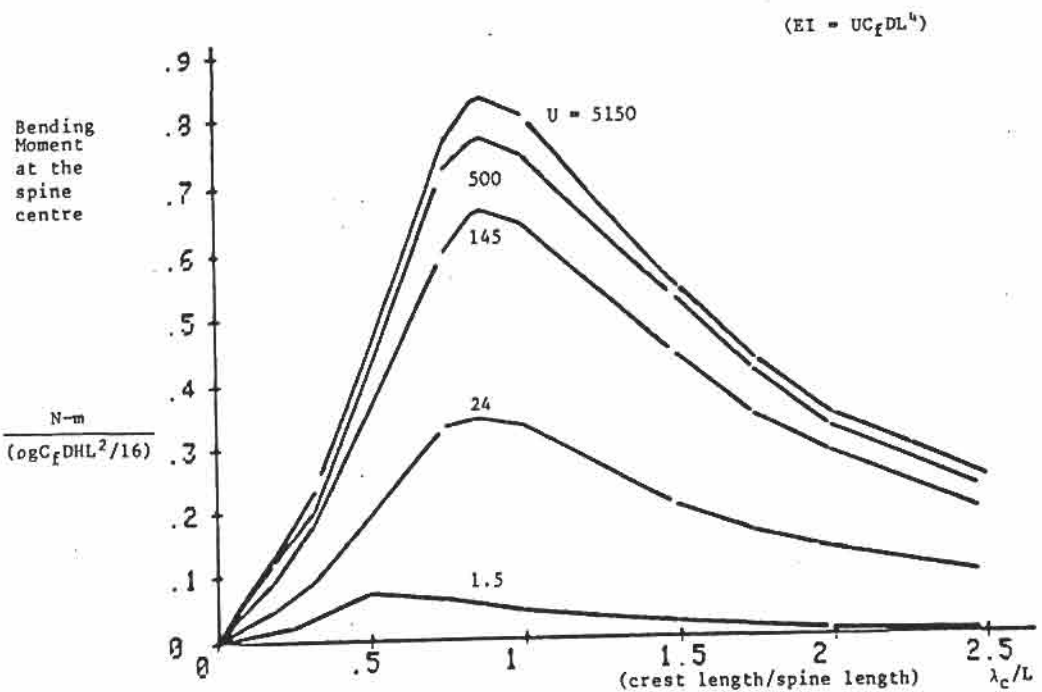

FIGURE 3 CENTRE BENDING MOMENT v λ_c/L FOR A RANGE OF STIFFNESSES

height within the record period could be predicted for a particular H_s and T_z case. Thus using these values of wave height and associated 'crest' length together with appropriate values of C_f from narrow tank tests (horizontal C_f = 0.35, vertical C_f = 0.27 suitable for most situations), the most likely maximum bending moment could be evaluated for any measured H_s. These values could be plotted on the bending moment v H_s curves and compared with experimental results.

This predicted most likely maximum bending moment curve has been compared with experimental results for the whole range of lengths, shapes and stiffnesses for which tests were carried out. (Typical curves, figures 4, 5, 6, 7, 8). The curves showed a nearly linear bending moment increase with increasing wave height, following closely the upper band of experimental values, then levelled off and started to reduce, now generally on a line above the upper bound of experimental results. The horizontal quasi-static predictions tend to over-estimate the maximum bending moments beyond the top of the curve, a fact which is felt to be partly due to an 'overtopping' effect when, for the low freeboard spines tested, the waves become large compared with the freeboard. Plots of peak horizontal bending moments v H_s for spines at angles less than 90 degrees to the principal wave direction are very similar in shape and magnitude to those for 90 degrees. Because angling the device has effectively reduced the 'crest' length, for a particular wave height, as seen by the spine, one would expect a larger wave to be able to induce an increased bending moment. However as the spine is angled to the principal wave direction, the magnitude of the horizontal wave forces is reduced by the incident angle cosine function, thus reducing the peak bending moment by a similar amount.

An interesting analysis derived from a note by Ewing to the Wave energy steering committee, (WESC (78) DA 66) is presented in graphical form in figure 9 and shows the effect on worst case horizontal bending moment of variations of 'crest' length to wave length ratio and device angle to the principal wave direction. The plot of (effective Hmax / device length) against device angle implies that the worst case effective wave height, and hence maximum horizontal bending moment, occurs at angles between 60 and 45 degrees to the principal wave direction for all reasonable 'crest' length conditions. Furthermore the difference between maximum values, in this range of 'crest' length conditions, is only about 10%.

The trends of figure 9 are borne out by the 1/10th. scale test results for different spine angles to principal wave direction which show that the maximum horizontal moment remains at much the same level for angles from 90 to 40 degrees.

Figure 9 would indicate some initial increase of maximum bending

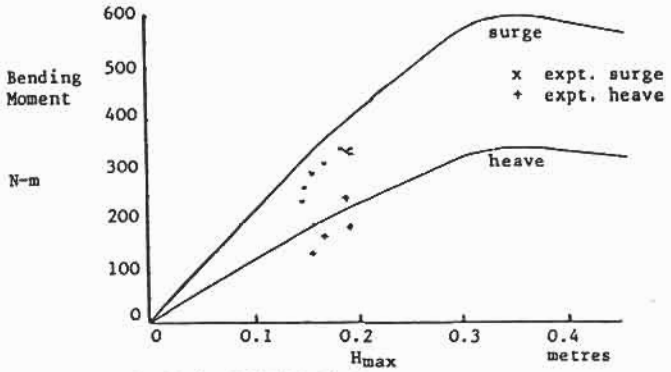

FIGURE 4 BENDING MOMENT v H_{max}
PREDICTED & EXPERIMENTAL DATA FOR 1/50th SCALE SPINE

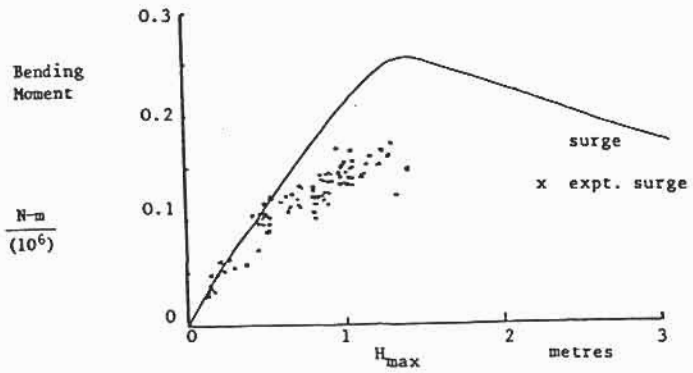

FIGURE 5 BENDING MOMENT v H_{max}
PREDICTED & EXPERIMENTAL DATA FOR 1/10th SCALE SPINE

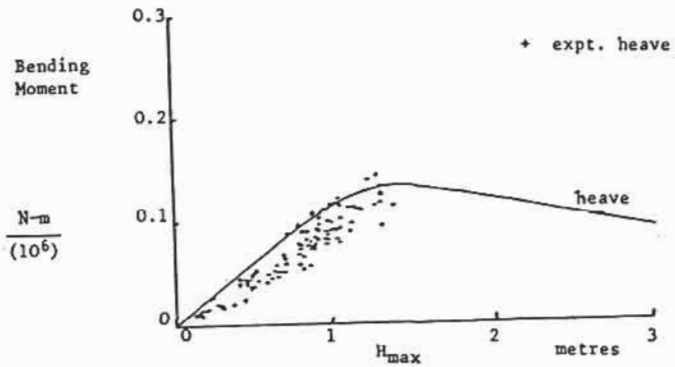

FIGURE 6 BENDING MOMENT v H_{max}
PREDICTED & EXPERIMENTAL DATA FOR 1/10th SCALE SPINE

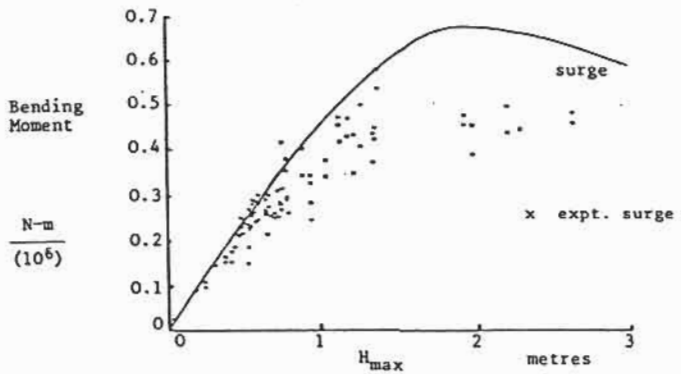

FIGURE 7 BENDING MOMENT v H_{max}
PREDICTED & EXPERIMENTAL DATA FOR 1/10th SCALE ACTIVE SPINE

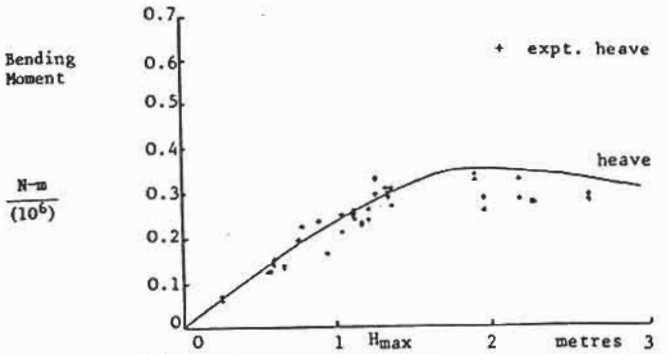

FIGURE 8 BENDING MOMENT v H_{max}

PREDICTED & EXPERIMENTAL DATA FOR 1/10th SCALE ACTIVE SPINE

Fig	Scale of expt.		Surge or Heave	C_f Value	Dimensions L metres	D	Stiffness parameter U	Active or passive spine
4	1:50	All	S	0.35	9.08	0.168	145	P
4	1:50	are	H	0.18	9.08	0.168	270	P
5	1:10	circu-	S	0.35	36	0.914	1510	P
6	1:10	lar	H	0.18	36	0.914	2780	P
7	1:10	spines	S	0.35	49.13	1.04	385	A
8	1:10		H	0.27	49.13	1.04	500	A

TABLE OF SPINE PROPERTIES, FIGURES 4-8

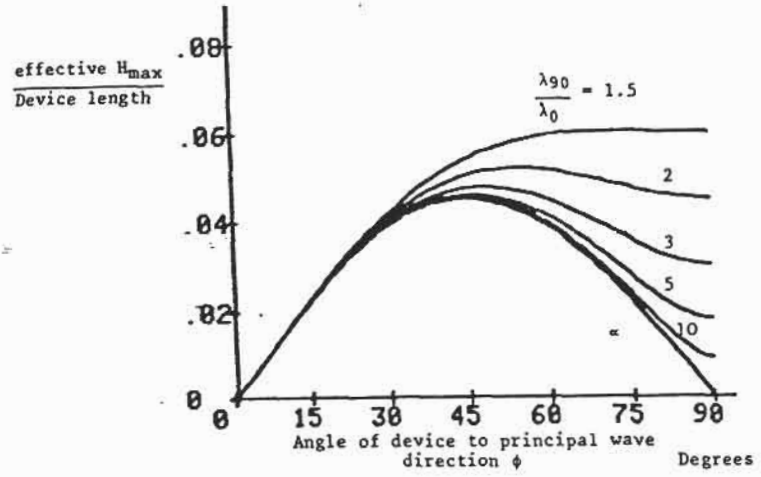

Effective $H_{max} = H_{max} \cos (90 - \phi)$

The worst wave height condition is defined as that at which crest length in the device direction = 0.9 x device length.
The worst wave length λ_0 is defined as = 10 H_{max}

According to Ewing[2], $\frac{\lambda_\phi}{\lambda_0} = (\cos^2\phi + \gamma^{-2} \sin^2\phi)^{-\frac{1}{2}}$

where $\gamma = \lambda_{90}/\lambda_0$

$\therefore \lambda_\phi = 0.9L = \lambda_0 (\cos^2\phi + \gamma^{-2} \sin^2\phi)^{-\frac{1}{2}}$

$= 10H (\cos^2\phi + \gamma^{-2} \sin^2\phi)^{-\frac{1}{2}}$

$$\therefore \frac{H_{max} \text{ effective}}{L} = \frac{0.09 \cos (90-\phi)}{(\cos^2\phi + \gamma^{-2}\sin^2\phi)^{-\frac{1}{2}}}$$

FIGURE 9 EFFECTIVE H_{max}/L v DEVICE ANGLE
FOR A RANGE OF CREST LENGTH-WAVE LENGTH RATIOS

moment as the spine angle goes down from 90 degrees, a trend not observed in the 1/10th. scale results. However two practical factors combine to cause the general level to remain the same. Firstly the range of experimental results for any angle cover an angular spread of about 20 degrees due to variations in principal wave direction and slow drift yawing of the spine. Secondly, as the spine angle reduces from 90 degrees the wave height necessary to cause the worst case bending moment increases and hence the overtopping effect becomes more pronounced with a corresponding reduction in the expected maximum moment.

Figure 9 also shows that substantial horizontal bending moments are still incurred even when the spine is close to the 'in line' position, a fact borne out by 1/10th. scale tests of a spine nominally at 0 degrees to the principal wave direction.

The quasi-static analysis implies that as the 'crest' length to spine length ratio goes beyond a limiting value the maximum horizontal bending moment is limited. This in turn implies a change in the peak bending moment to r.m.s. bending moment ratio as the wave heights increase and the limiting comes into effect more often within a recording period. Figure 10 is a plot of the peak to r.m.s. ratio for a 1/10th. scale rectangular spine of 27 m length, the mean line of the peak to r.m.s. ratio shows a definite decrease as H_s increases when compared with that expected using the Longuet-Higgins distribution for the particular record length.

BENDING MOMENT PREDICTION USING THE QUASI-STATIC METHOD.

It is possible to use the information presented in this paper to predict peak bending moments as follows:

Decide upon the worst case λ_c/H_{max} ratio which might be expected.
(We have used $\lambda_c = 30\ H_{max}$ at Loch Ness)

Substitute this into parameter λ_c/L on the x-axis of figure 3. (This gives a $30\ H_{max}/L$ axis for Loch Ness.)

Using values of $30\ H_{max}/L$ chosen from the axis at appropriate points, evaluate bending moment along a given stiffness curve.

Eg The stiffness curve in figure 3 marked 5150 peaks at 0.82 at approximately $30\ H_{max}/L = 0.9$
Bending moment for this condition is thus:

$$0.82 \times \left(\frac{\rho g C_f D L^2}{16}\right) \times \left(\frac{0.9L}{30}\right)$$

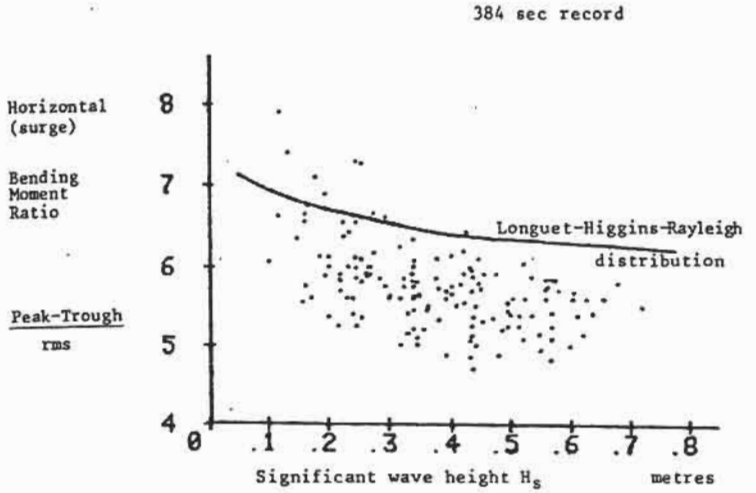

FIGURE 10 1981 LOCH NESS EXPERIMENTAL DATA
FROM 27m LONG RECTANGULAR SPINE (1/10th SCALE),
MOORED WITH EXTENSION IN PORT RODE
SPINE MAKING ANGLE OF 50°-60° WITH PRINCIPAL WAVE DIRECTION

Assuming ρ=1025 and C_f=0.35 in surge, bending moment is $5.4DL^3$ at this point.

A similar calculation for 30 H_{max}/L = 1.0 and 2.0 gives bending moments of $5.9DL^3$ and $5.1DL^3$ respectively. Note that peak bending moment does not coincide with the peak of the original curve of figure 3.

Using the above method, the value of 30 H_{max}/L and hence of H_{max} giving a bending moment peak can be established, and used in figure 2 to derive bending moment distribution along the spine.